

## **Wind Measurement with a Wind Profiling Radar**

*Qi Rundong, Huang Changcheng and Tian Wenbin*

Beijing Institute of Radio Measurement, P. O. Box 3923, Beijing 100854, China

(Received September 14, 1990)

**Abstract**—The first troposphere wind profiling radar in China has been in operation. The paper describes the radar parameters and characteristics with some experimental results presented.

**Keywords:** Pulsed Doppler radar, Wind profiler, Wind measurement.

### **1. Introduction**

Observations of radar returns which could not be attributed to aircraft or precipitation were referred to as “angels” or “ghosts”. It was conjectured that they had the possible origins of some mysterious targets. Only in the early 1970’s it became clear by a large amount of experimental investigations that these returns were ascribed to two types of targets: (1) Discrete targets such as insects and birds; (2) Distributed targets, mainly the inhomogeneities of the atmosphere refractive index which cause backscattering and reflection.

In researches on the causes of clear-air echoes, advance is made by two advanced instruments: highly sensitive pulsed Doppler radar [Dobson, 1970; Browning et al., 1972] and high-resolution (non-Doppler) FM-CW radar [Richer, 1969].

Since 1970, the pulsed Doppler radar has made great advances. A dual-Doppler system was able to sense two components of the wind in the boundary layer over a  $25 \times 25$  km area [Doviak and Jobson, 1979]. Around 1980, the wind measurement of the atmosphere could be made by using a VHF / UHF pulsed Doppler radar, while clear-air echoes were researched by using pulsed Doppler radars. The UHF wind profiling radar researched by NOAA WPL<sup>[1]</sup> has been put into use. The troposphere wind profiling radar, jointly developed by the Beijing Institute of Radio Measurement and the Chinese Academy of Meteorological Science is now in service.

### **2. Radar Returns due to Incoherent Scattering from Refractive Index Inhomogeneity**

In 1960s, the researchers made the satisfactory explanations for most of clear-air phenomena by electromagnetic scattering theory in turbulence medium. Tatarski, one of the most remarkable scientists, deduced the formula of computing electromagnetic scattering in turbulence medium by using the fundamentals of Kolmogorov’s part isotropic turbulence. It agrees

with the experimental results.

The primary cause of clear-air echoes in the atmosphere is scattering from refractive index inhomogeneity. The radio refractive index depends mainly on air temperature and water vapor pressure. In the upper troposphere the water vapor pressure is small, and only temperature gradients make a significant contribution to refractive index gradients. In the lower troposphere the refractive index is more sensitive to humidity.

Ottersten described the general relationship between radar reflectivity  $\eta$  and refractive index variations. Under certain simplified conditions [Hardy et al., 1966], the reflectivity is related to  $C_n^2$ , the refractive index structure constant, defined as the RMS difference in refractive index at two points unit distance apart. The radar reflectivity is expressed by

$$\eta = 0.38 C_n^2 \lambda^{-3} \quad (1)$$

The assumptions are as follows:

—The inhomogeneities caused by the turbulence should be isotropic and should uniformly fill the radar resolution volume.

—One half the radar wavelength must fall within the inertial subrange.

—No other targets such as insects, cloud droplets, or specular reflection should contribute to the reflectivity.

When scattering medium fills the radar resolution volume, the radar equation can be described as

$$P_r = \frac{P_t A_e L^2 c \tau}{16\pi R^2} \cdot \eta \quad (2)$$

where  $P_r$  is the received echo power of receiver input terminal,  $P_t$  is the transmitted peak power,  $A_e$  is the effective antenna area,  $c$  is the light speed,  $\tau$  is the pulse width,  $\eta$  is the radar reflectivity,  $L$  is the transmission efficiency.

The backward scattering echoes produced by refractive index variation is very weak for VHF-UHF radar. The scattering medium is distributed almost continuously in the atmosphere. The scattering echoes vary quickly with time and the time scale of variance corresponds to the scale of turbulence variance.

### 3. Wind Measurement of the Atmosphere

The first troposphere wind profiling radar in China, CFL-86, was developed in 1986. Located at Daxin county of Beijing suburb, the radar functions well.

#### 3.1 Fundamentals of wind measurement

As shown in Fig.1, three fixed antenna beams are used by the CFL-86 wind profiling radar. The antenna is an electrically steered phased array antenna. Three antenna beam-pointing directions are needed to measure the vector wind. For simplicity, the pointing directions are chosen to observe orthogonal and horizontal wind components  $u$  and  $v$ , and the vertical

component  $w$ . The antenna elevation pointing angle is  $Q_e$ . When the radar transmits the electromagnetic wave along the antenna beam—pointing direction, it will produce backward echoes varying with the wind of atmosphere. The echo is received by the radar receiver, then the Doppler wind velocity is analyzed by signal processing and the wind is computed at various heights of interest. Because the echo signal from scattering of clear-air atmosphere is very weak, it is necessary to use large-aperture antennas, high average power and low noise receivers and long time integration.

When the radar operates, the computer controls the antenna to scan sequentially each of three beam-pointing directions. The horizontal wind profiles can be made after horizontal components  $u$  and  $v$  and the vertical component  $w$  are computed.

The radial Doppler velocities  $V_i$  measured by the radar are related to the wind as follows:

$$\begin{aligned} V_1 &= u\cos\theta_e + w\sin\theta_e \\ V_2 &= v\cos\theta_e + w\sin\theta_e \\ V_3 &= w \end{aligned}$$

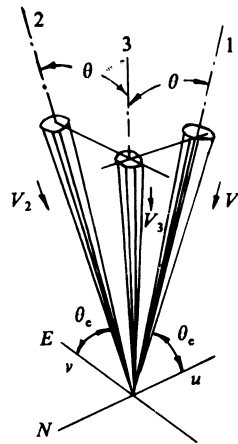


Fig.1 Schematic diagram of CFL-86 radar antenna beam positions

In Fig.1 the antenna azimuth angles for  $V_1$  and  $V_2$  are  $0^\circ$  and  $90^\circ$ , respectively.  $V_1$ ,  $V_2$  and  $V_3$ , the three measurements are made at volumes separated in space at the height  $h$ . Horizontal uniformity is assumed when the measurements are combined.

### 3.2 Radar system description

The CFL-86 radar consists of phased Yagi antenna array and driver, transmitter, receiver and frequency synthesizer, monitor, radar controller and signal processor, computer, modem and radio communication equipment.

It works at UHF band, the frequency is 365 MHz. The radar characteristics and operating parameters are listed in Table 1 and Table 2 respectively. Fig.2 is the block diagram of the radar.

The antenna array consists of 108 Yagi antennas with 5 elements, each of them phased by the PIN phase shifter. The antennas are set in octagon for limiting the sidelobes and getting higher gain. The antenna array aperture is about  $7\text{m} \times 8\text{m}$ . The two-way beam width is  $7^\circ$ .

The transmitter has three stages. The peak power is 22 kW. The transmitter operates with a maximum duty factor of 3% with the pulse length from 1 to 9  $\mu$ s. The receiver is an all-coherent receiver, with a dynamic range of 60 dB (IF). T / R switch is a PIN diode. The receiver noise figure is 2 dB.

**Table 1. CFL-86 radar characteristic**

Frequency	365 MHz
Peak power	22 kW
Duty	<3%
Antenna aperture	7m $\times$ 8m
Antenna pointing	zenith, 15 $^{\circ}$ off-zenith to east and south
Two-way beamwidth	7 $^{\circ}$
Receiver noise figure	2 dB

**Table 2. CFL-86 radar operating parameters**

	Mode 1	Mode 2	Mode 3
Data processing			
Pulse width	1 $\mu$ s	3 $\mu$ s	9 $\mu$ s
Pulse repetition period	100 $\mu$ s	150 $\mu$ s	300 $\mu$ s
Time domain averaging	120 pulses	90 pulses	40 pulses
Spectral averaging	16	16	24
Spectral resolution (128 points)	0.268ms $^{-1}$	0.238ms $^{-1}$	0.268ms $^{-1}$
Height sampling			
First height	200m	1.5km	4km
Height spacing	100m	300m	900m
Number of sampling heights	24	24	13

The radar controller, a 80286CPU, is designed for programmed time control and system monitoring. The signal processor TMS32010 performs the spectral analysis.

The radar terminal computer, a PC / AT, performs the estimation of spectral moments, combination of wind field, graphic display and data transmission. A high resolution CRT with 640  $\times$  400 pixels displays the radar status, profiles of moments and wind profiles in real time.

### 3.3 Signal and data processing

The signal and data processing is shown in Fig.3.

The three moments of the Doppler spectra are estimated: signal power  $P$ , mean radial velocity  $V_r$ , and spectrum width  $W$ . The signal-to-noise ratio (SNR) is computed from the

Doppler spectrum. The signal received is the backscattered signal for each radar resolution cell. The receiver amplifies the signal and limits the bandwidth with a filter matched with the transmitted pulse. After coherent detection the complex video signal is transferred to A / D. The complex video signal represents the composite amplitude and phase of the scattering process in the radar resolution volume.

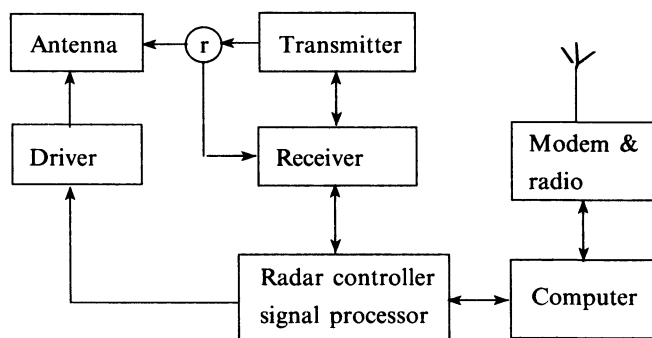


Fig.2 Block diagram of the CFL-86 radar

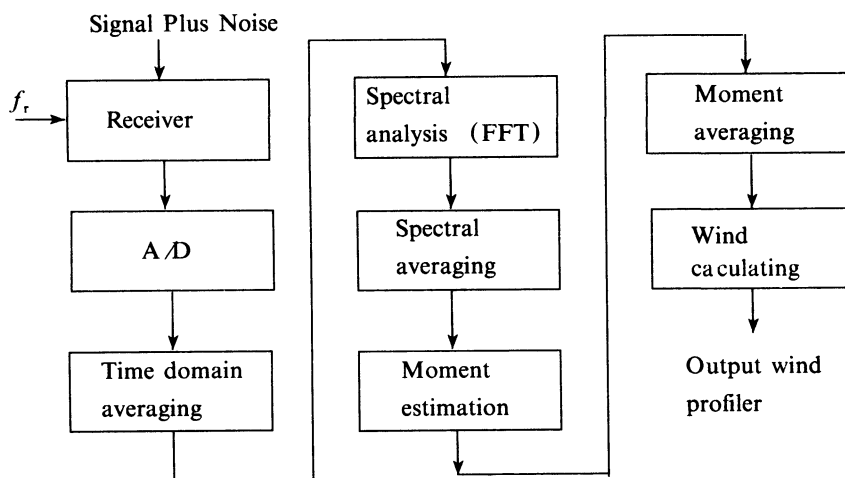


Fig.3 Signal and data processing steps

The sampled signal is integrated by time domain averaging with two purposes: (1) improving the SNR, (2) minimizing the calculation burden. Since the noise bandwidth is determined by the radar pulse width and noise samples taken in the pulse repetition period are uncorrelated, the noise power increases linearly with the number of samples added. However, the signal correlation time for an UHF radar is a few seconds. The phase of the signal samples changes very little during consecutive sampling and the signal power increases with the square of the number of samples added. The SNR is improved to the number  $J$  of samples added, and the unambiguous velocity decreases to  $\lambda / (4JT)$ , where  $\lambda$  is the radar wavelength,  $T$  is the pulse repetition period.

The next step in signal processing is spectral analysis. The SNR improvement factor is

given by  $K \operatorname{erf}(\Delta V / 2\sqrt{2W})$  in FFT of  $K$  samples<sup>[1]</sup>, where  $\Delta V$  is the velocity resolution and  $W$  is the signal spectral width. For a small  $K$  the improvement factor increases linearly with  $K$ ; for a large  $K$ , the improvement factor increases little with  $K$ . The next processing step is the averaging of  $L$  spectra. For each dwell time  $T_D = JKT$ , SNR increases by  $\sqrt{L}$  if the mean wind is the same. If the mean wind is not the same, then the width of the averaged spectrum increases during the averaging and SNR improvement will be less than  $\sqrt{L}$ . To get the improvement in SNR by taking full advantage of spectral averaging,  $L$  should be limited to about  $d / (JKT \bar{v})$ , where  $d$  is the maximum dimension of the observation volume (beam width or range resolution, whichever is greater) and  $\bar{v}$  is the mean wind velocity.

Now, we get the averaged spectra. Then, the spectral moments can be estimated from the Doppler spectra. Before estimating the moments, the signal must be separated from the noise. Because fixed clutter of DC offsets in the spectrum, the *half plane subtraction* method is used for removing the clutter and zero frequency signal.

The *partial averaging* method is used to estimate the noise level. That is, the spectrum is cut into  $M$  parts, then the minimum value is found from the  $M$  parts. This value is taken as the mean noise level. After determining the noise level, the signal spectrum should be isolated by using the subset separation method. This can be done as follows. First, all the subsets including those contiguous spectral points that exceed the mean noise are isolated, then the subset of which total addition of all points is maximum is taken as signal spectrum. The classical definition of the moments is then applied to the isolated signal spectrum. This method seems to be well suited to a wide variety of conditions.

Finally, estimates of spectral moments can be averaged by using a simple version of random sample consensus. The radial profiles of mean velocity at all heights are obtained, and then horizontal wind profiles are combined from them.

### 3.4 Samples of measurement

The CFL-86 radar began to operate in November, 1988. Fig.4 shows the results of wind profiles observed on September 22-23, 1989. The first and 13th columns were the results of balloon sounding for comparison with the results of radar observation. It took the radar 30 minutes to obtain a profile. Though the wind direction field changed little between 19:00 and 01:00, it changed from southwest to south for a short time within the five hours at a 3 km height. Fig.5 shows the wind velocity and direction profiles observed on August 31, 1989.

Fig.6 makes comparisons between the results of radar observation and the results of balloon sounding.

## 4. Summary Discussion

In this paper we have described briefly the troposphere wind profiling radar. The technique of wind sounding will make great advance by using the profiling radar. According to the state-of-the-art, an advanced atmospheric sounding system should be constituted by the VHF and UHF wind profiling radars, microwave radiometers and Radio Acoustic Sounding System (RASS).

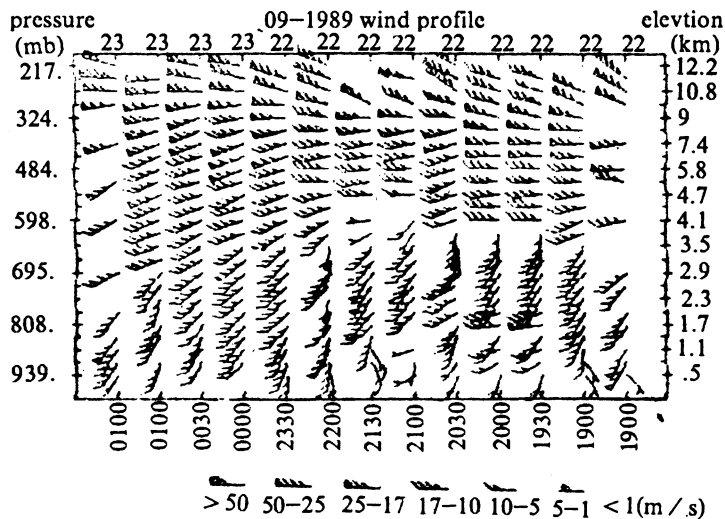


Fig.4 Data samples measured every 30 min by the CFL-86 rader

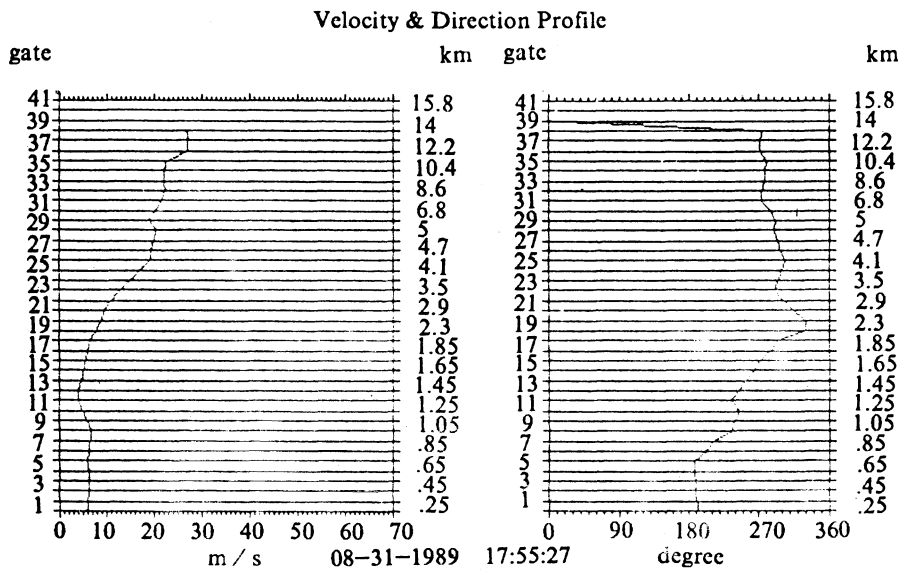


Fig.5 Data samples of the observed wind velocity and direction

The RASS is used for remotely determining the atmospheric temperature profiles by combining acoustic and radar techniques. It has been successfully applied to the wind profiling radar<sup>[5],[6]</sup>. Tian Yalong who works at Chinese Academy of Meteorological Science has successfully made the RASS experiment on the CFL-86 wind profiling radar. In the future, wind profilers will measure the clear air signal as well as the RASS signal, making possible

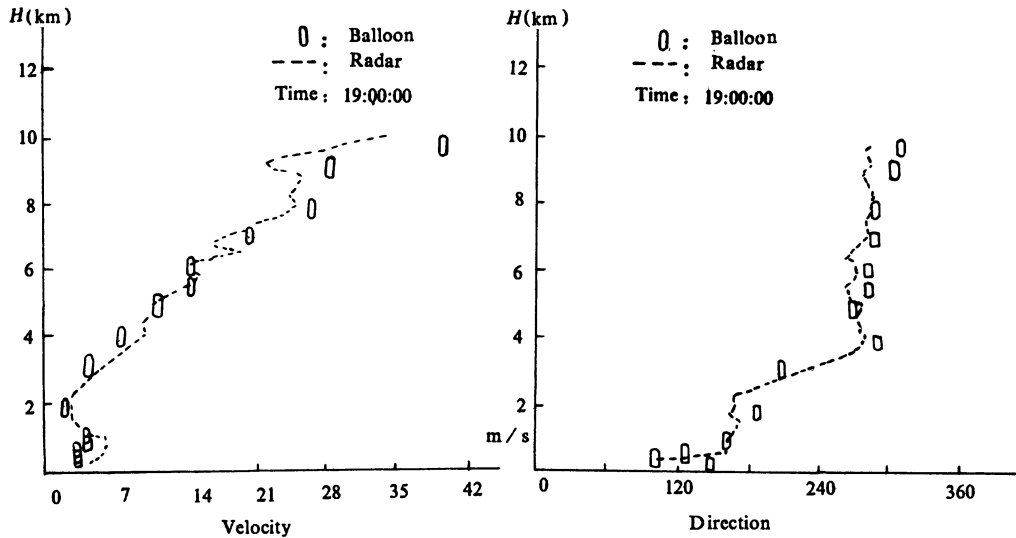


Fig.6 Results of radar observation in comparison with the results of balloon sounding (August 10, 1989)

simultaneous measurements of wind and temperature.

### Acknowledgments

We extend thanks to our colleagues for their cooperation and support. We also wish to acknowledge Ma Daan and Zhao Chonglong from CAMS for their contributions to our study.

### References

- [1] R. G. Strauch *et al.*, "The colorado wind-profiling network", *J. Atmospheric and Ocean Technology*, 1984.
- [2] P. K. James, "A review of radar observations of the troposphere in clear air conditions", *Radio Science*, Vol. 15, 1980.
- [3] K. R. Hardy, "Multiwave-length backscatter from the clear atmosphere", *J. Geophys. Res.*, 1966.
- [4] W. L. Ecklund *et al.*, "A UHF wind profiler for the boundary layer: brief description and initial results", *J. Atmospheric and Ocean Technology*, 1988.
- [5] P. J. May, R. G. Strauch *et al.*, "Temperature sounding by RASS with wind profiler radar: a preliminary study", *IEEE. T-GE*, Vol. 28, No.1, 1990.
- [6] Tian Yalong, RASS system research with UHF wind profiling radar. Postgraduate thesis, Chinese Academy of Meteorological Science, 1990.